



Estimation of Bluefin Tuna (*Thunnus thynnus*) mean length in sea cages by acoustical means

V. Puig-Pons^{a,*}, P. Muñoz-Benavent^b, I. Pérez-Arjona^a, A. Ladino^a, S. Llorens-Escrich^a, G. Andreu-García^b, José M. Valiente-González^b, V. Atienza-Vanacloig^b, P. Ordóñez-Cebrián^c, José I. Pastor-Gimeno^a, V. Espinosa^a

^a Institut d'Investigació per a la Gestió Integrada de Zones Costaneres (IGIC), Universitat Politècnica de València (UPV), C/Paranimf 1, 46730 Gandia, Spain

^b Institute of Control Systems and Industrial Computing (AI2), Universitat Politècnica de València (UPV), Camí de Vera (s/n), 46022 València, Spain

^c Zunibal S.L., Idorsolo Kalea, 1, 48160 Derio, Spain

ARTICLE INFO

Article history:

Received 26 January 2022

Received in revised form 30 May 2022

Accepted 27 July 2022

Keywords:

Underwater acoustics

Bluefin Tuna Biomass estimation

Underwater computer vision

Target strength

Fish management

Fish sizing

ABSTRACT

This paper proposes an indirect method to estimate Bluefin Tuna (*Thunnus thynnus*) biomass in cages using acoustic techniques. Two Simrad EK60 echosounders working at 120 and 200 kHz and a stereo camera were used to obtain target strength (TS) to fork length (FL) relationships for both operating frequencies. The equipment was placed at the bottom of a floating cage, facing towards the surface to record the ventral aspect of fish. The acoustic and optical recordings were automatically analysed and the combination of acoustic and optical results provided unequivocal TS-FL assignments. Good relationships between TS and FL were obtained for both frequencies even without discriminating data from different fish tilts and without using beam directivity compensation. Stronger correlations were obtained for compensated TS at 200 kHz when reduced tuna swimming tilt was considered. TS measurements were compared to MFS numerical predictions for a Bluefin swimbladder model, with the simulation results showing good agreement with experimental measurements. The results allow the mean tuna length to be predicted in growing or fattening cages from acoustic data raising the possibility of improving production management and of providing a useful tool for catch control estimations made by international organisations (like ICCAT) and government bodies.

© 2022 The Author(s). Published by Elsevier Ltd. This is an open access article under the CC BY-NC-ND license (<http://creativecommons.org/licenses/by-nc-nd/4.0/>).

1. Introduction

Atlantic Bluefin Tuna (*Thunnus thynnus*) is a highly valued specie (both economically and ecologically) that has become endangered in recent decades from overfishing. For this reason, the International Commission for the Conservation of Atlantic Tunas (ICCAT) implemented a recovery plan, enforcing three major rules: to establish a fishing quota, to impose a closed fishing season and a minimum catch size (30 kg). Some signs of stock recovery resulting from these efforts have been reported [1].

* Corresponding author at: Institut d'Investigació per a la Gestió Integrada de Zones Costaneres (IGIC), Universitat Politècnica de València (UPV), C/Paranimf 1, 46730 Gandia, Spain.

E-mail addresses: vipuipon@upv.es (V. Puig-Pons), pmunyo@upv.es (P. Muñoz-Benavent), iparjona@upv.es (I. Pérez-Arjona), anlave@upv.es (A. Ladino), sulloes@upv.es (S. Llorens-Escrich), gandreu@upv.es (G. Andreu-García), jvalient@upv.es (J.M. Valiente-González), vatiensa@upv.es (V. Atienza-Vanacloig), patricia.ordonez@zunibal.com (P. Ordóñez-Cebrián), jpastogi@upv.es (J.I. Pastor-Gimeno), vespinos@upv.es (V. Espinosa).

Atlantic Bluefin Tuna (ABFT) capture-based aquaculture generated about 40,000 tons of fattened tuna in 2018 in the world (compared to more than 60,000 tons in 2005) [2–4]. Catch estimation and control, as well as production management, calls for sizing and biomass estimation techniques. ABFT ranchers also need tools to control the fattening process, thus helping them improve tuna production efficiency in sea cages. Furthermore, recent successes in Bluefin Tuna closed loop aquaculture have shown the future need for monitoring their growth. In addition, all of the stakeholders are debating on how to improve the control mechanisms of fishing quota [1].

Nowadays, ABFT catch and production controls in tuna fattening sea cages are carried out either by manual sampling or by using stereoscopic cameras systems. The former can harm the fish and increases costs for farmers, while the latter is non-intrusive for tuna but it is affected by water depth and turbidity, as well as limited camera's observation volume [5,6]. The most widely used commercial stereoscopic systems are AQ1 AM100 [7] and AKVAsmart VICASS [8]. These systems are manual or semi-automatic

and require human operators to inspect the pair of videos (or photographs). The process is as follows: the fish snout and fork in both stereo images should be marked manually to estimate tuna length. In both frames, tuna must be isolated and straight. Some attempts have been made to improve their performance and capability of automation [9,10,11,12]. Indeed, recently, Muñoz-Benavent et al. [13] presented a fully automatic procedure based on a stereoscopic system (using a deformable model of ABFT proposed in [14,15] to obtain ABFT length without human intervention. However, this technique needed a large number of recorded images from the ventral tuna aspect to give very accurate results but increasing the processing time.

Besides video recordings, acoustic techniques have been widely used in ecological fish research and for fish assessment [16]. In fact, they are one of the most effective and non-intrusive methods to obtain a fish biomass estimation. To do so, individual acoustic response or target strength (TS), is used. TS is defined as the ratio of backscattered and incident acoustic intensities. The TS value depends on the size of fish, its behaviour, its internal physiology, its morphology, the orientation of its body with respect to the transmitted beam, the presence and state of swimbladder [16–18] (Foote et al., 1987; Furusawa, 1988; Simonds and MacLennan, 2007) and on the acoustic frequency. TS is used as a decisive scaling factor for estimating fish abundance and the relationship between TS and fish length has been established for a large number of fish species [16,19]. There are TS studies available in literature including in situ TS of Yellowfin Tuna (YFT) (*Thunnus albacares*) and Bigeye Tuna (*Thunnus obesus*) [20,21], and ex situ measurements of YFT in a tank have been presented by [22]. More recently Melvin in his work [23] measured in situ dorsal TS from 34 ABFT with a 120 kHz echosounder. The mean TS value obtained in that study was -20.4 dB but no length information was available for the individual fish. All these studies were performed from a dorsal perspective of fish.

TS measurements have also been proposed for monitoring fish growing in aquaculture floating cages, and particularly TS recordings from the ventral aspect, that is, with the ultrasonic transducer placed at the bottom of the cage facing the sea surface. Knudsen et al. in [24] showed an excellent correlation of ventral TS with Atlantic salmon length (*Salmo salar*). This result is especially relevant, since TS measurements in cages can be affected by a variety of errors associated with the distances involved: near field effects for the emitted and backscattered fields, partial insonification of the fish, relative size of fish compared to the insonified volume, and finite transducer size, time-varying-gain accuracy, etc. [25–28]. Recently, numerical simulations of the experimental conditions of TS measurements performed by [24], allowed the differences between close TS measurements of the dorsal and the ventral aspect of fish to be interpreted in terms of the necessary distance to overcome the influence of the near field of the scattered wave [29]. The shadowing effect of fish bone on the swimbladder, in the case of dorsal measurements, resulted in longer near field distances than in the ventral case. This could justify the conclusions given by [24], which suggested ventral TS measurements for monitoring fish growth in aquaculture cages, where echosounding is restricted by the farming facilities' dimensions.

The objective of this work is to establish a relationship between ventrally measured target strength (TS) and fork length (FL) for ABFT in floating cages which can be a useful tool for catch control estimates and production management. Tuna length in fattening cages may vary between the minimum allowed size (30 kg or 115 cm approximately) and the maximum length determined for ABFT by [30] that has been established at 331 cm. Since the variation of fish size is very high, the only possibility of extracting a correlation of fish size with TS is to simultaneously measure the size

of the insonified fish, which is possible from the ventral perspective following the technique given by [13].

ABFT fattening cage dimensions are limited (usually 30 m deep), and therefore measurements must be carried out considering the related issues at close distances. Following the definition TS and the standard methods to measure it [16,17], one must achieve complete insonification of the scatterer, that is, a wide enough beam aperture and a long enough pulse duration to guarantee that the fish fits into the volume insonified by the acoustical pulse. The measurements must be done in a distance where far field condition of the transducer is ensured. Moreover, measuring distance must guarantee that the backscattered field has evolved to its final far field shape when it is detected by the echosounder. These conditions are difficult to fulfil completely, with the distances and typical fish sizes like those described above. Other sources of error related to the point-like violation and the directivity compensation made by scientific echosounders are also present. In this work, we performed preliminary tests to define the acoustical methodology to assign ventral TS values to ABFT in cages. Our tests concentrated on adjusting the acoustical parameters to focus on the swimbladder's response. Recent works have underlined the role of swimbladder (when present) as the major contributor to backscattered acoustic energy, and the convenience of reducing fish size to its swimbladder size to evaluate near field effects [31].

Taking into account the aforementioned fish sizes (and their corresponding swimbladder), we also considered it necessary to investigate numerically of the near field effect of tuna, considering the interplay of swimbladder size and the transducer directivity. Several numerical methods have been used in the past to evaluate the TS of fish for both idealised and realistic models [18,32,33,34,35,36,37]. A comparison of different numerical methods to calculate TS can also be found in [38] and [39], for the case of swimbladdered fish. Nevertheless, most of those models are restricted to use at distances far enough to be in the far-field region, which is acceptable for most study cases, except for the particular situation with short distances and/or large targets when the evolution of the ultrasonic field over distance could be relevant. In such cases, numerical methods like finite element method (FEM) or boundary element method (BEM) can be used to estimate TS, but, as we know [38], these methods require high computing demands at high frequencies. The method of fundamental solutions (MFS) has been verified as a suitable method for estimating the measured TS of fish at arbitrary distances in the far field from the transducer, and it can be used to understand the features of the near field of the fish. Indeed, MFS has been tested against the most recognized numerical methods, exhibiting better performance in computational terms than BEM or FEM for smooth geometries [29].

Assuming all the experimental restrictions and error sources, we have investigated the possibility of performing the acoustical estimation of mean length for Bluefin Tuna catches transferred to floating cages and therefore also the viability of tuna growth monitoring in aquaculture for which automation is an added value.

2. Materials and methods

2.1. Experimental setup for data acquisition

Measurements were taken place from July to October 2015 in three floating cages in production conditions installed on the Mediterranean Spanish coast at L'Ametlla de Mar ($4^{\circ}05'21.7''$ N and $0^{\circ}48'15.2''$ E). Approximately 650 ABFT (caught by a purse-seining fleet in May 2015) were housed in cages each with a diameter of 50 m and a maximum depth of 35 m. Recordings were made one day a month in each cage from July to October.

Two Simrad EK60 echosounders with split-beam transducers working at different frequencies (120 and 200 kHz) were used for the TS measurements. Both transducers (ES200-7C and ES120-7C) have a nominal angle of 7°. The on-axis and off-axis calibration (for both echosounders) was carried out using the standard calibration method. A 23 mm diameter copper sphere was used to calibrate the 120 kHz system and a 13 mm copper sphere to calibrate the 200 kHz echosounder [40]. The acoustical setup was a matter of preliminary tests, and also a configuration with a 200 kHz single beam transducer with 31° of beam width used. Some results and considerations about the different beam apertures and pulse lengths are given below. The parameters finally used are given in Table 1.

To obtain a relationship between tuna length and ventral TS, the acoustic system was linked to a stereoscopic camera system (AM100, AQ1Systems), which consists of two Gigabit Ethernet cameras, with image resolution of 1360x1024 pixels and framerate of 12 fps. The cameras are mounted in an underwater housing, with a baseline of 80 cm and an inward convergence of 6°.

The transducers and cameras were mounted on a platform (Fig. 1) such that they recorded the ventral views of tuna, enabling ventral TS measurements and ABFT fork length calculation [13]. The optical system also enabled the tuna tilt angle to be estimated. In this case, the tilt angle corresponds to the angle between the tuna's body axis and the plane defined by transducers' surfaces. The platform was placed at the cage bottom (19 m deep) with sensors facing the surface. Due to tuna behaviour observed in [41], the equipment was placed in the middle of the radius (12.5 m from the net cage) in order to increase the number of tuna detections.

Table 1
Parameters of acoustic systems (Simrad EK60) and filtering parameters used to detect single targets.

	120 kHz	200 kHz
Echosounder system		
Ping interval (s ⁻¹)	17	17
Transducer gain (dB)	23.86	24.48
Transmitted pulse duration (ms)	0.064	0.064
Power (W)	100	90
Two-way beam angle (dB)	-20.7	-20.7
Minor axis 3dB beam angle (°)	6.20	6.35
Major axis 3 dB beam angle (°)	6.25	6.41
Single target detection		
Minimum TS threshold (dB)	-40	-40
Minimum echolength ratio with pulse duration	0.4	0.4
Maximum echolength ratio with pulse duration	4	4
Maximum phase deviation	3	3
Maximum gain compensation (dB)	12	12

2.2. Measurement of fork length

The fully automatic procedures given by [13] and [15] was used to obtain a high amount of accurate FL values. The procedures consist of applying the following steps to the recorded stereoscopic videos. Firstly, image segmentation using local thresholding is performed and the segmented regions are geometrically characterized and sifted using appropriate aspect ratio, pixel density and dimensional filters. Afterwards, an edge detection algorithm is applied and a geometrically deformable tuna model is fitted to the fish's silhouette. Finally, 3D measurements are computed using the calibration parameters and 3D triangulation, in fish with guaranteed stereo correspondence.

2.3. Bluefin Tuna swimbladder properties and 3D modelling

As mentioned in the Introduction, recent works emphasize the convenience of reducing fish size to its swimbladder size to evaluate near field effects, as it was the major contributor to backscattered acoustic energy.

ABFT swimbladder shape, orientation and size are not very well documented, but the swimbladder properties of Yellowfin tuna (YFT) have been described in some works [42]. YFT swimbladder has a particular shape, but it can be approximated by with a prolate spheroid of a size close to one-fifth of total tuna length. Schaefer and Oliver [42] observed an inclination around 25° to the backbone, which is consistent with the results from acoustic measurements made in tanks [22], obtaining maximum values of backscattering when YFT shows an inclination near to this value.

To study the ABFT swimbladder properties, different X-ray tomographies were analysed. Firstly, we obtained a computerized axial X-ray tomography of a frozen ABFT caught by longlines, where the swimbladder appeared partially deflated and deformed, but with a length at least a sixth of fish fork length (for a specimen of 113 cm). However, information about the shape was not conclusive in that image. Using the CSI (Computerized Scanning and Imaging Facility) of the Woods Hole Oceanographic Institution, we also obtained another X-ray scan of a 60 cm long ABFT (see Fig. 2), which gave a swimbladder proportion of 1/4 of fork length, with a shape that could be described as a composition of two prolate spheroids with a maximum diameter of 1/5 of height of fish, tilted 20° to the backbone. For insonification purposes, for these data we assumed typical values for swimbladder size and a ratio 1:5 for swimbladder length compared to fork length of tuna well as for the swimbladder diameter compared to the height of tuna. Under these assumptions, a swimbladder of a 2 m tuna should be totally insonified at 0.72 m and 3.3 m for a -3 dB beam width of 31 and 7°, respectively. Moreover, minimum pulse duration of 64 μs should allow us to identify the backscatter from the

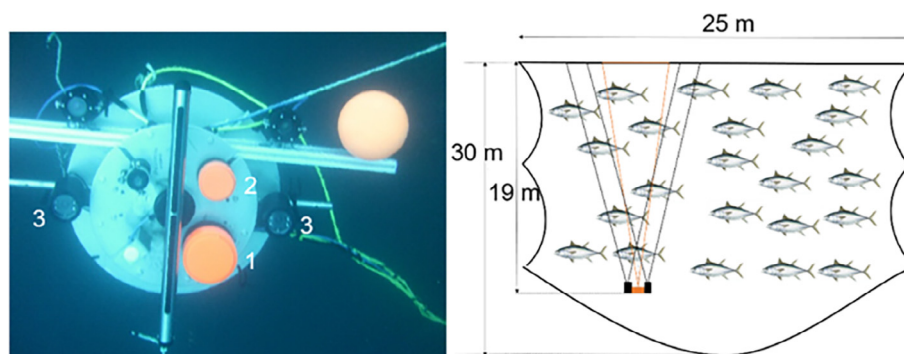


Fig. 1. Experimental setup. Underwater platform (left) 120 kHz transducer (1), 200 kHz transducer (2) and stereoscopic camera system (3). Setup diagram (right): Equipment at the bottom facing the surface.

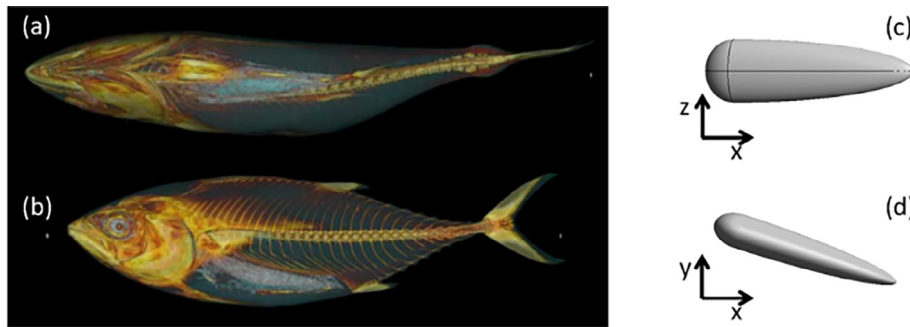


Fig. 2. Left: 3D tomographic images of an ABFT individual from the CSI (Computerized Scanning and Imaging Facility) at the Woods Hole Oceanographic Institution with XZ (a) and XY (b) planes. XZ (c) and XY (d) planes of the ABFT swimbladder model's geometry considered.

flesh-gas interface of swimbladder, separated from the signals from the others structures.

The tomographic images of ABFT were considered to develop a 3D model of Bluefin Tuna swimbladder. Fig. 2 shows XY and XZ planes of the 3D tomographic image and the corresponding XY and XZ planes of the considered MFS model, being Z the beam propagation direction and X axis the head-to-tail fish direction. The smooth geometry of the swimbladder model (Fig. 2b) allows to take profit of the computational advantages of MFS [29]. The number of collocation points used to solve the model was $\lambda/6$, being λ the wave length.

2.4. Methodology for ventral TS measurements

In order to design the acoustical experimental setup, taking into account the availability in our laboratory of EK60 echosounders, we tested different transducers beam widths and emitted pulse lengths in tuna cages: two beam widths (31° and 7° at -3dB) and minimum and maximum pulse duration ($64 \mu\text{s}$ and $1024 \mu\text{s}$). The use of 31° beam width would allow to insonify completely a 2 m long tuna at a distance of 3.6 m, whilst the 7° one at 16.4 m. Tuna heights in fattening cages can reach more than 60 cm [43–45] and therefore maximal pulse duration should be desirable to integrate fish completely.

Acoustic data were analysed using digital image processing of echograms, since the final selected configuration provided complex-looking traces. If a Single Echo Detection (SED) algorithm was applied it resulted in a complex fish track structure, i.e., it could not be reduced to a single linear track. Echograms were converted to binary images, and morphological operations were used to obtain closed regions and to remove noise. Finally, a region-based segmentation was implemented. Size threshold and TS threshold (-40 dB) were imposed to separate tuna traces from other target traces. Such a TS threshold was selected attending on TS-versus-length relationship found in the work by [22] and mean TS value obtained by [23]. In [22] study, a linear regression between TS and fork length for YFT was given using a 200 kHz echosounder in a tank. The minimum ABFT length in the studied fattening cages was about 120 cm, which corresponded to a TS of -28.77 dB applying [22] free slope TS-FL equation (-30.86 using fixed slope equation) For each trace, maximum TS value (compensated and uncompensated) was obtained. Fig. 3 shows the necessary steps of the echogram processing method to obtain an isolated trace from the recorded raw data.

2.5. Optical-acoustic correspondence and TS-FL relationship

When the tuna body was completely straight and inside the beam (Fig. 4), the maximum ventral TS (from the echogram analysed), length and tilt angle (from the paired images from the

stereoscopic system) of ABFT were recorded. The stereo system was only capable of measuring up to a maximum distance of 10 m because, at greater distances the error in length estimation increased. For this reason, only tuna that crossed the acoustic beam between 4 and 10 m were measured. This resulted in unique TS-FL data pairs, ensuring that the registered acoustic energy came from the tuna that was measured in the pair of images.

In this paper we propose both compensated and uncompensated maximum ventral TS versus fork length relationships, according to the linearized equation:

$$TS = a \log(FL) + b \quad (1)$$

where a is a slope and b is the intercept. Both are constants related to species and fish behaviour (mainly changes in fish tilt angle). The free slope was used (instead of a fixed slope as is used in other studies [46]) to provide a better TS-FL fit; we obtained both the slope and intercept that correlated the experimental values of TS with optically measured length for ABFT in cages.

2.6. Numerical simulations of measured target strength in the near field of Bluefin Tuna

MFS numerical predictions of TS measurements were performed for the previously defined ABFT swimbladder model. The swimbladder was considered as a pressure release surface surrounded by sea water with material properties given by volumetric density $\rho = 1027 \text{ kg/m}^3$ and longitudinal sound speed $c = 1479 \text{ m/s}$, insonified by a high frequency acoustic beam.

The acoustic beam was described as the far field of a circular piston with a half-beam angle at -3dB of 3.5° , as an idealisation of an echosounder acoustic transducer [29], fitting the transducers' specifications of Simrad EK60 scientific echosounders at 120 kHz.

The numerical estimations considered tuna fork length $FL = 120 \text{ cm}$ and 200 cm at $f = 120 \text{ kHz}$. Calculations performed at 70 kHz and 120 kHz allowed the frequency response to be considered, though evaluations at higher frequencies required higher memory capabilities than available.

The aforementioned tomographic images of ABFT were considered to develop a 3D model of ABFT swimbladder, as the main contribution to the value of fish TS.

2.7. Estimation of the influence of pulse duration on the target strength measurements

The scattering properties of a target can be decomposed into two contributions: the effective area that intercepts the acoustic wave (or apparent cross-section seen from the echosounder, $A(\theta_i)$), and the directional characteristics of the scatterer, that result in a scattering function depending on the incident and scattering directions ($G(\theta_i, \theta_s)$). A simple figure of a general scheme is given

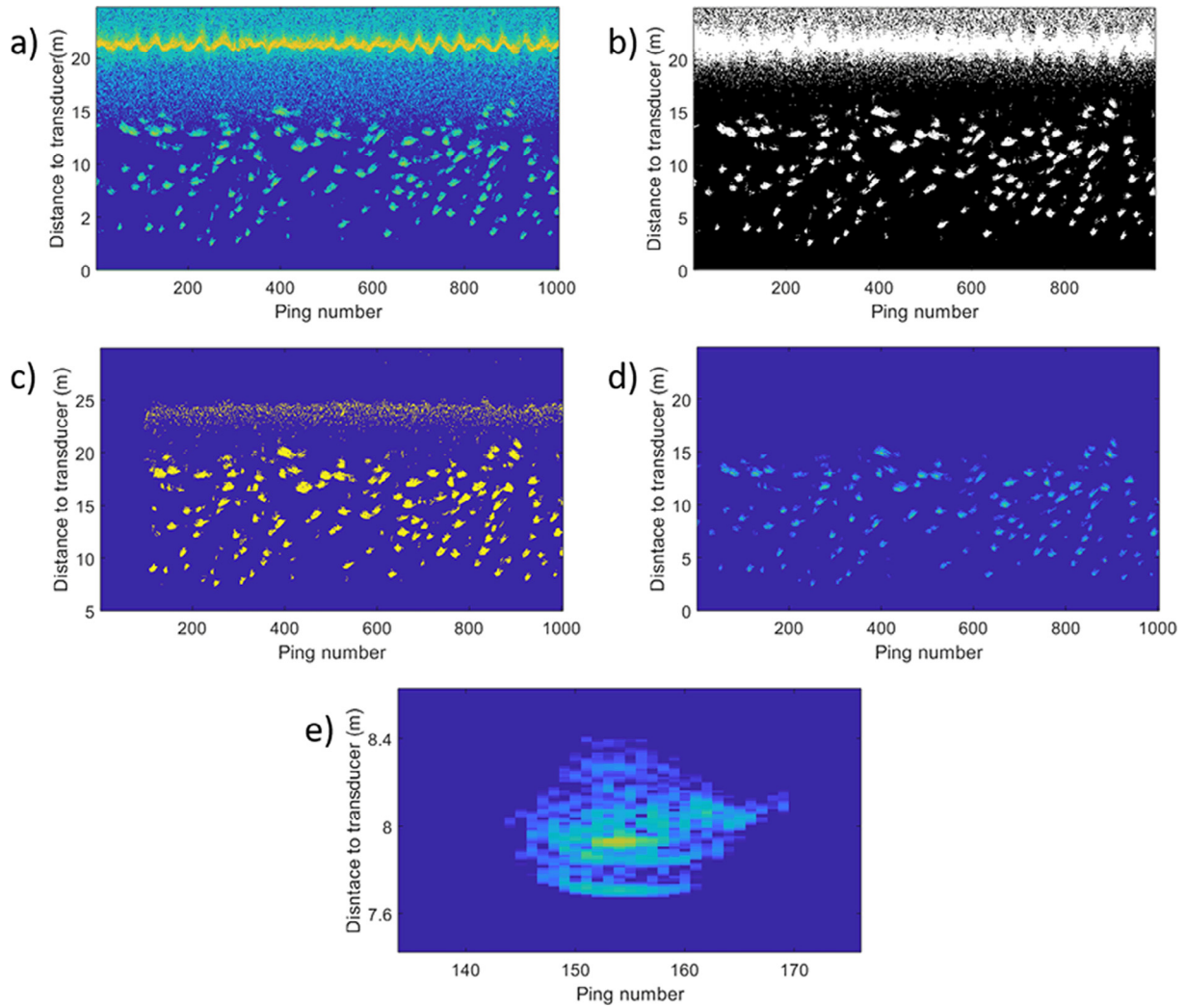


Fig. 3. Image processing techniques used. a) Echogram recorded. b) Image binarization and morphological operation used (opening algorithm to remove noise, thickening to obtain compact regions and closing algorithm to fill small holes). c) Region-based segmentation. d) Size threshold and TS threshold applied. e) Isolated trace from this echogram.

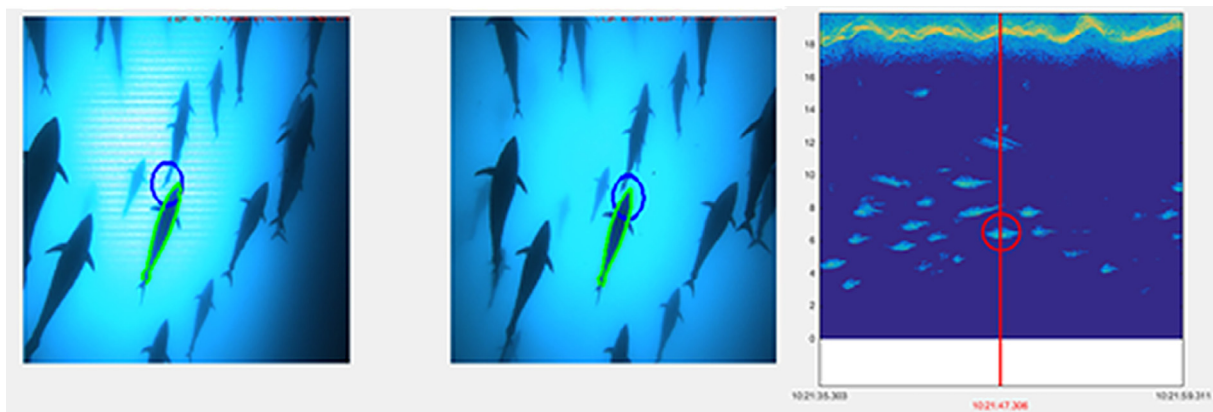


Fig. 4. Data processing image: On the left, images from stereoscopic system, the blue circle corresponds with acoustic beam. Straight tuna crossing the acoustic beam is measured. On the right we can see an echogram, the red line marks the acoustic trace corresponding with images (red circle). (For interpretation of the references to colour in this figure legend, the reader is referred to the web version of this article.)

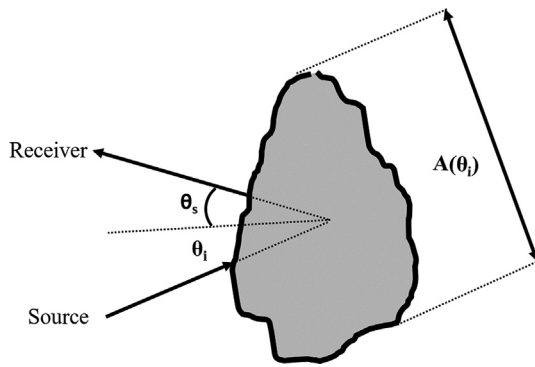


Fig. 5. Scheme of incident and scattering directions (θ_i, θ_s) and apparent cross-section $A(\theta_i)$.

in [47] (Figure 3.8 therein) which is depicted in Fig. 5. The effective scattering cross section [47] (pages 71–72) of the target is then expressed as:

$$\sigma(\theta_i) = A(\theta_i) \cdot G(\theta_i, \theta_s) \tag{2}$$

Assuming that the main contribution to the TS of Bluefin Tuna is given by the swimbladder, and considering that the incidence and scattering direction are the same to the echosounder ($\theta_s = \theta_i$), the measured TS would be directly dependent on the value of the maximum apparent cross-section of the swimbladder from this direction. This maximum cross section can only be achieved if the emitted pulse is long enough to insonify completely the target from the first hit until the maximum body section. In order to estimate the influence of pulse duration on the observed TS, we consider a simplified model of this organ, a prolate spheroid of semi axis a and b . The maximum apparent cross-section of this body, insonified with a plane wave travelling in the direction parallel to its minor semi-axis a , corresponds to the area of the ellipsoid defined by a and b :

$$A = \pi ab \tag{3}$$

This maximum apparent cross-section would intercept a plane wave with a pulse duration allowing to insonify at least a half of the prolate spheroid, corresponding to an insonification length $c \tau/2$ equal to a . For smaller pulse durations, the apparent cross section would be reduced to the ellipsoid area reached by the insonification length $e = c \tau/2$, A_r , as depicted in the inset of Fig. 6, and given by:

$$A_r = A \left(1 - (a - e)^2 / a^2 \right) \tag{4}$$

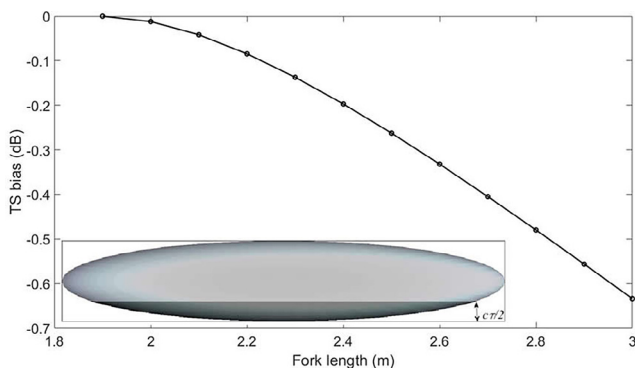


Fig. 6. TS bias (underestimation) plotted as a function of BFT fork length for a pulse duration of $64 \mu s$. The inset shows the geometrical scheme of the insonified volume for a pulse duration of value τ .

The estimated TS bias for a determined pulse duration, will result from the comparison of A_r to A . This estimation will be calculated in the following section for the selected pulse-length experimental setup.

3. Results

3.1. Preliminary tests on beam width and pulse duration

The results of the tests are summarized in Figs. 7 and 8. In principle, the maximum beam width of 31° allowed tuna to be completely insonified in almost in the whole measuring range, while the minimum width of 7° could only insonify the swimbladder in an equivalent distance range (Fig. 7c and 7f). The echogram obtained with the 31° beam width showed multiple trace superimposition even at close distances, severely affecting the trace isolation capability in the water column, as can be seen in Fig. 7a and 7b, and making it almost impossible with the longer pulse duration (Fig. 7a). In the echogram obtained with the 7° beam, individual traces can be observed more easily but they appear to be superimposed at closer distances with the longer pulse duration of $1024 \mu s$, making it difficult to apply automatic trace extraction using the image processing method explained in the Method section above. In Table 2 we have summarized the capability of automatic analysis of traces in the echograms as a function of beam aperture and pulse duration. The number of tuna traces that can be extracted in an echogram of 5 min of duration decreases severely.

as pulse duration increases.

Fig. 8 shows four examples of individual echogram traces for a typical tuna fork length of 2 m, recorded with the mentioned configurations (31° and 7° each with the 64 and $1024 \mu s$ pulse durations). The selected traces were taken at a distance of between 3 and 4 m from the 31° transducer (Fig. 8a and 8b) and at approximately 7 m from the 7° one. The traces in Fig. 8a and 8b have the typical “v” shape, whilst those in Fig. 8c and 8d are significantly shorter. The inner structure of the traces is clearly more complex for the pulse duration of $64 \mu s$, whereas traces recorded with the maximum pulse duration are more homogeneous. Together with the echogram traces we have depicted the corresponding echo envelope for the ping of maximum amplitude within the trace, which is expected when the swimbladder is insonified. Echo envelopes for $1024 \mu s$ show a monotonous variation from the echo start to its maximum value and later decay, whilst echo envelopes for $64 \mu s$ allow us to identify a main contribution to the echo level within the fish dimensions’ limits, with similar maximum TS values to those obtained for the $1024 \mu s$ traces.

Considering these results, and to assure the maximum degree of automation of the future monitoring system the acoustical set up for our TS measurements was selected, and 7° beam width with split beam transducers were used with a pulse duration of $64 \mu s$.

This choice was made with a certain concern about its possible influence on TS measurements. TS measurements can be affected by pulse duration as studied in [48]. In section 3.3 we offer the results of the numerical simulation of TS, including the possible effect of the near field of fish. In addition, an estimation of the possible TS bias, introduced by the choice of pulse duration, is given in section 3.4.

3.2. Results of ventral TS measurements

There were 3,295 ABFT single traces were detected for the 120 kHz operating frequency in accordance with the paired images from stereo video system providing the corresponding fork length. In the same way, 3,505 traces were found at 200 kHz. The fork length distributions (Fig. 9c and 9f) ranged between 120 and

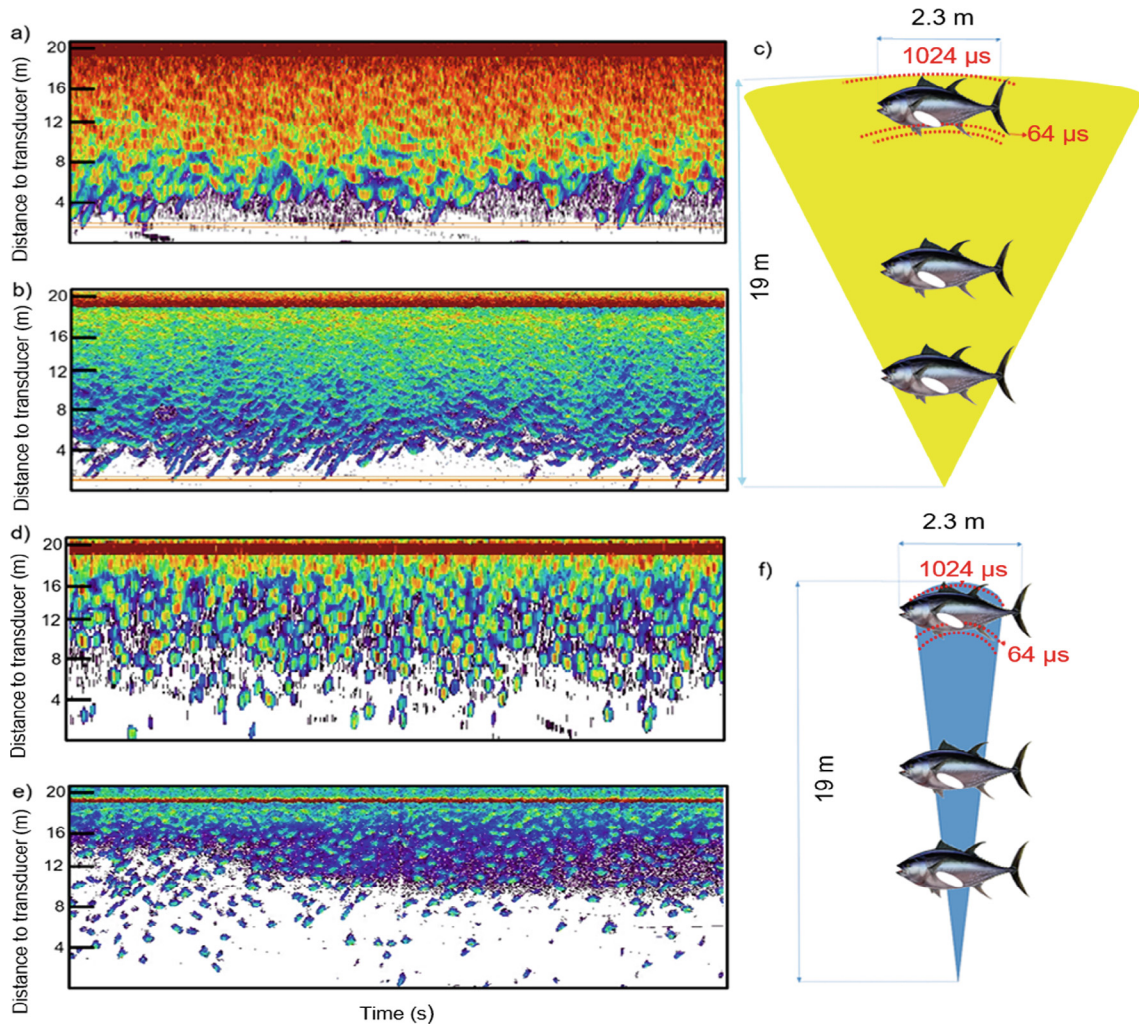


Fig. 7. a) 1024 μs pulse duration echogram (acoustic beam size of 31° (Simrad ES10 at 200 kHz). b) 64 μs pulse duration echogram (acoustic beam size of 31° (Simrad ES10 at 200 kHz). c) Diagram of tuna body and swimbladder insonification for 64 μs and 1024 μs pulse duration and acoustic beam size of 31° (Simrad ES10). d) 1024 μs pulse duration echogram (acoustic beam size of 7° (Simrad ES200-7C at 200 kHz). e) 64 μs pulse duration echogram (acoustic beam size of 7° (Simrad ES200-7C at 200 kHz). f) Diagram of tuna body and swimbladder insonification for 64 μs and 1024 μs pulse duration and acoustic beam size of 7° (Simrad ES200-7C).

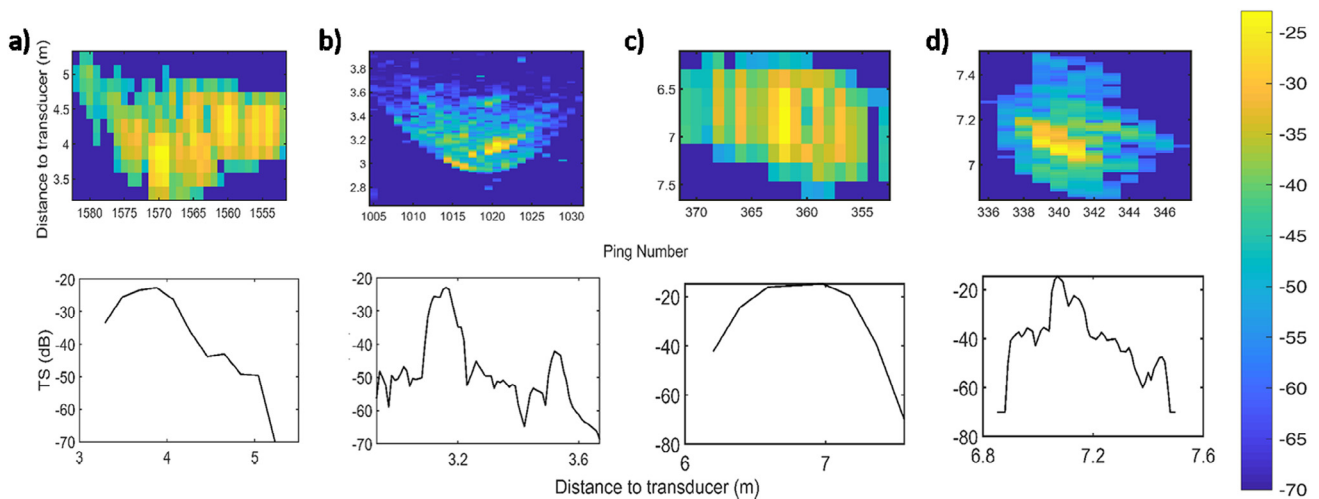


Fig. 8. a) Echogram trace of a single tuna (above) and temporal envelope of the ping with maximum echo TS within (below); 1024 μs pulse duration and acoustic beam size of 31° (Simrad ES10 at 200 kHz). b) Trace and envelope for 64 μs pulse duration for the same beam size of 31° c) Trace and envelope for 1024 μs pulse duration and acoustic beam size of 7° (Simrad ES200-7C at 200 kHz), d) Trace and envelope for 64 μs pulse duration for the same beam size of 7°.

Table 2
Number of traces extracted automatically for each transducer in 5 min echogram.

Transducer (beam aperture)	Simrad ES10 (31°)			Simrad ES200-7C (7°)		
Pulse duration (μs)	64	256	1024	64	256	1024
Number of isolated traces	117	40	8	397	200	34

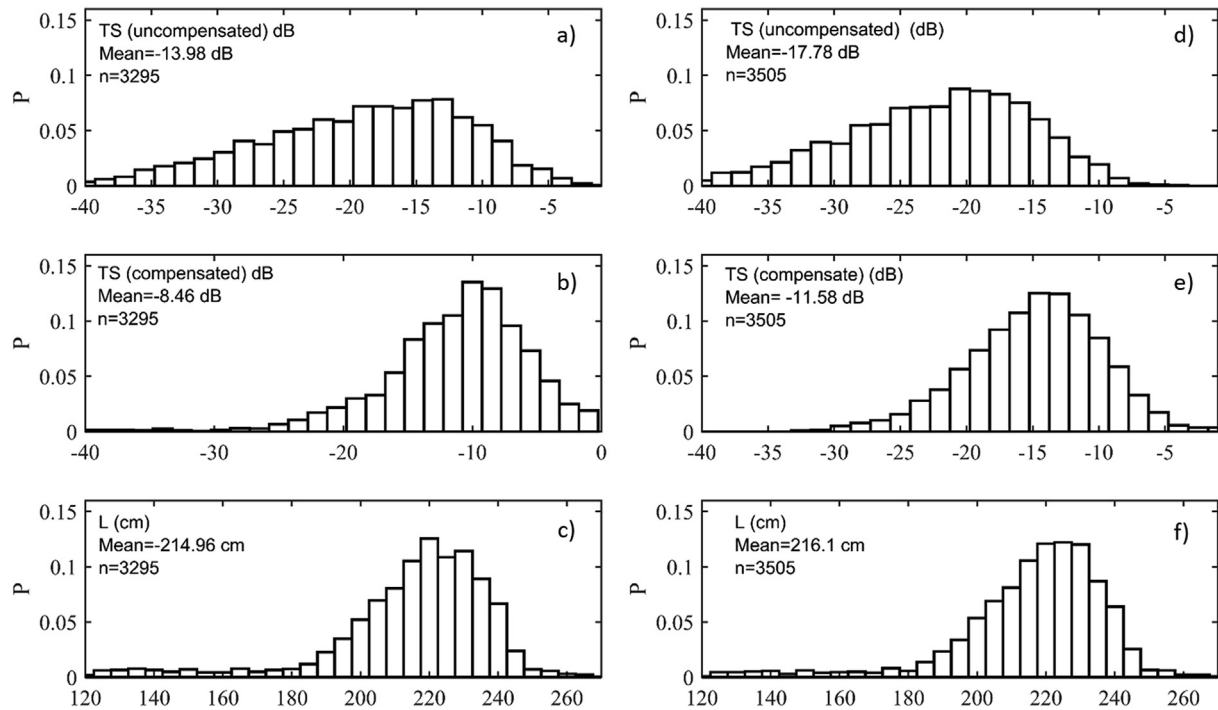


Fig. 9. a) Probability density distribution of uncompensated TS at 120 kHz. b) Probability density distribution of compensated TS at 120 kHz. c) Probability density distribution of inferred ABFT fork length at 120 kHz. d) Probability density distribution of uncompensated TS at 200 kHz. e) Probability density distribution of compensated TS at 200 kHz. f) Probability density distribution of ABFT fork length at 200 kHz.

170 cm (for corresponding traces at both operating frequencies). Two major modes were observed for measurements at 120 kHz centred on 220 and 230 cm. Only one mode (225 cm) was seen for image pairs at 200 kHz. Both length distributions obtained had a coefficient of variation (CV) of 11 %.

The 120 kHz ventral TS distribution (for uncompensated and compensated maximum TS within each trace, Fig. 9a and 9b respectively) exhibited a value range from -40 to -1 dB. The same applied to 200 kHz (Fig. 9d and 9e). For both frequencies, histograms of uncompensated TS were more widely distributed (Fig. 9a and 9b), with a CV of 78 % (120 kHz) and 83 % (200 kHz), versus 46 % and 30 %, respectively. The mean value and major mode were higher for 120 kHz (average TS: -13.98 dB and mode: -13 dB) than for 200 kHz (average value: -17.78 dB and mode: -19 dB). The average TS value for 120 kHz (Fig. 9b) was 3 dB above average TS for 200 kHz (around 3 dB).

Data analysis of acoustic-optical correspondences allowed us to observe that the most probable orientation in the cage was a tilt angle of fish in the 0° to 2° interval as indicated by the mode value of the probability density in Fig. 10, but maximum amount of TS versus FL assignments was concentrated between -5° and 5°.

To obtain a significant correlation between TS (dB) and logarithmic ABFT fork length (for both frequencies), TS-FL correspondences were grouped into 10 cm intervals of tuna length. Mean value of TS was calculated for each group and these values were fitted using a linear regression. The linear regression fits are summarized in Table 3 and Table 4. In the case of 120 kHz (Table 3), from the R² value, the best fit was found for the first group of tilt interval,

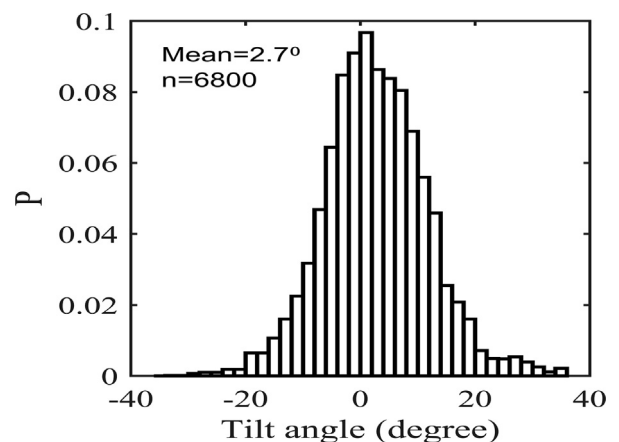


Fig. 10. Swimming tilt angle of the ABFT obtained from optical system for all acoustic-optical correspondences found at 120 and 200 kHz.

[-5° 5°], and in the last group, [-35° 35°] for the uncompensated TS case. Generally, the slopes had lower values in compensated TS. The 200 kHz frequency fits gave slightly different results, with generally lower linear slopes (Table 4). The best correlations were obtained in the first group only in the compensated TS case. However, uncompensated TS (200 kHz) also showed the best fit in the last group [-35° 35°]. In Fig. 11 scatterplot TS-length relationship has been shown. At the top of the Fig. 11 compensated and uncom-

Table 3

Summary of the parameters from linear regression of TS versus length grouped by tuna orientation at 120 kHz. The asterisks show the level of significance in the F-test analysis of variance for the model: ** for $p < 0.01$, * for $0.01 < p < 0.05$ and if $p \geq 0.05$, the value is shown.

TS (dB)=a·log ₁₀ FL (cm)+b f=120 kHz									
Tuna tilt interval group	number	uncompensated TS		R ²	Significance	compensated TS		R ²	Significance
		a	b			a	b		
[-5° - 5°]	1236	24.33	-70.87	0.71	**	20.97	-57.48	0.74	**
[-10° - 10°]	2092	25.90	-74.47	0.70	**	23.68	-63.94	0.60	**
[-20° - 20°]	2776	25.56	-73.72	0.64	**	24.42	-65.49	0.57	**
[-35° - 35°]	3295	24.77	-71.57	0.72	**	18.79	-52.53	0.67	**

Table 4

Summary of the parameters from linear regression of TS versus length grouped by tuna orientation at 200 kHz. The asterisks show the level of significance in the F-test analysis of variance for the model: ** for $p < 0.01$, * for $0.01 < p < 0.05$ and if $p \geq 0.05$, the value is shown.

TS (dB) = a·log ₁₀ FL (cm) + b f = 200 kHz									
Tuna tilt interval group	number	uncompensated TS		R ²	Significance	compensated TS		R ²	Significance
		a	b			a	b		
[-5° - 5°]	1271	12.01	-45.55	0.54	$p \approx 0.05$	21.14	-61.28	0.85	**
[-10° - 10°]	2184	12.69	-47.51	0.67	*	19.63	-58.02	0.83	**
[-20° - 20°]	2849	17.11	-57.64	0.62	**	11.94	-40.00	0.47	**
[-35° - 35°]	3505	14.95	-52.64	0.62	**	12.85	-42.12	0.58	**

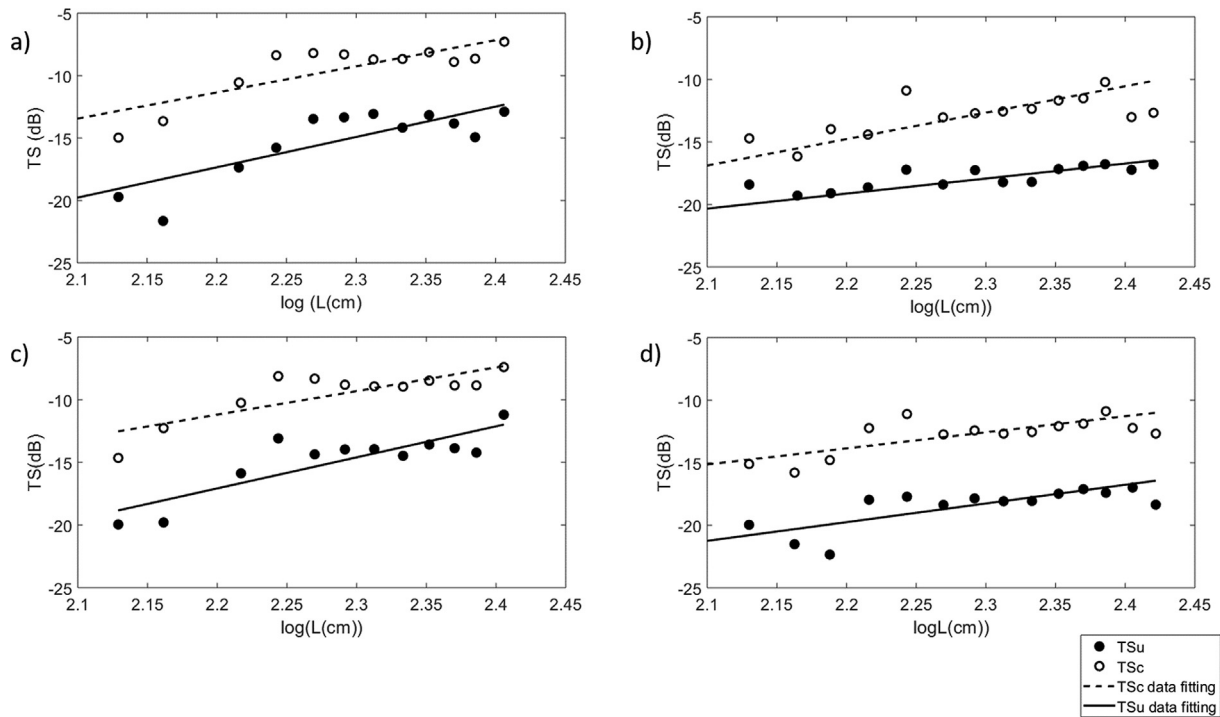


Fig. 11. a) Scatter plot and fitting result of compensated and uncompensated TS at 120 kHz for a [-5° 5°] tilt interval group. b) Scatter plot and fitting result of compensated and uncompensated TS at 200 kHz for a [-5° 5°] tilt interval group. c) Scatter plot and fitting result of compensated and uncompensated TS at 120 kHz for a [-35° 35°] tilt interval group. d) Scatter plot and fitting result of compensated and uncompensated TS at 200 kHz for a [-35° 35°] tilt interval group.

compensated TS-length scatterplot, obtained within a tilt interval [-5° 5°], for both frequencies are presented. At the bottom part the last tilt interval group [-35° 35°] at 120 and 200 kHz has been shown.

The dependence of TS measurements on the fish distance to transducer was studied for both frequencies. To do so, TS measurements of tuna whose fork length was between 220 and 230 cm were considered. This group contained the largest number of acoustic-optical correspondences, with 777 matches for 120 kHz and 882 for 200 kHz. The average TS value in one-meter layers was calculated from 4 to 9 m to the transducer surface. The average TS included all possible tuna orientations contained in the [-35°, 35°] interval. If we focus on 120 kHz (Fig. 12a), TS dependence with

distance was observed in compensated and uncompensated TS cases. The average TS values (compensated and uncompensated) increased with the distance to the transducer. Differences of up to 4 dB between nearest and farthest point were found in both cases. At 200 kHz (Fig. 12b) the same situation occurred for uncompensated TS but compensated TS shown less direct dependence with distance (about 1 dB).

Finally, with the aim of predicting average tuna length in a cage from acoustic data, the mean TS in a measurement layer from 5 to 10 m from the transducer was calculated and presented in Table 5. In order to know the mean tuna length in the cage, Grup Balfegó provided data of fish lengths collected on harvesting (Table 5).

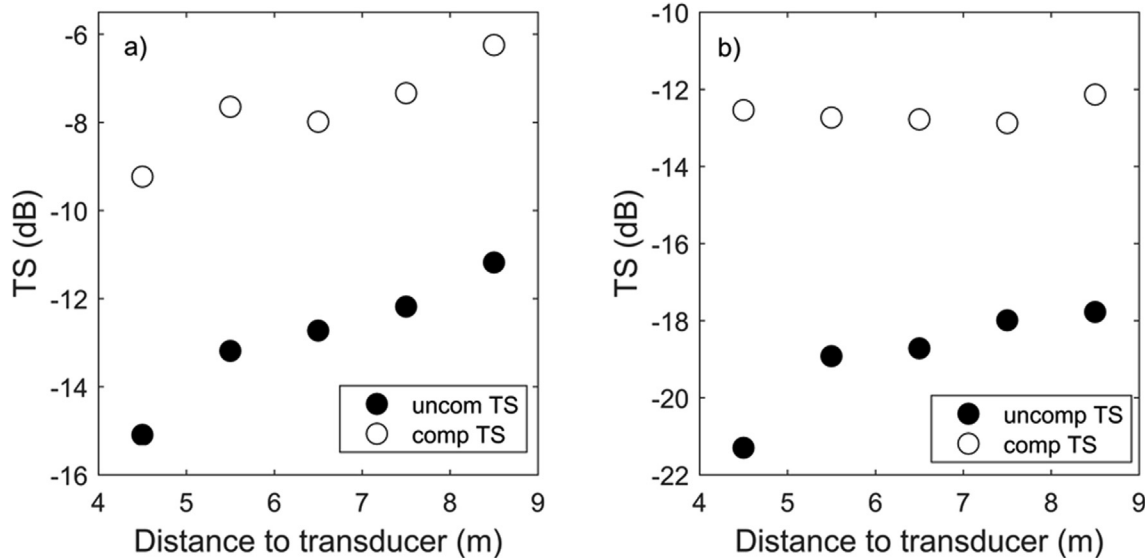


Fig. 12. Plot of TS versus depth for the 220 to 230 cm group of tuna length: a) 120 kHz data; b) 200 kHz data.

Table 5

Mean maximum TS (compensated and uncompensated) in layer studied. Mean length predicted from acoustic data using linear regressions shown in Tables 2 and 3 for the [-5° to 5°] orientation interval. Error (deviation) between the calculated mean length and data of mean length from measurements taken during the tuna harvest.

	uncompensated TS		compensated TS	
	120 kHz	200 kHz	120 kHz	200 kHz
Mean maximum TS (dB)	-14 ± 11	-18 ± 14	-8 ± 4	-12 ± 3
Mean L (cm) predicted	208 ± 2	209 ± 5	212 ± 2	223 ± 2
Mean L (cm) harvests	220 ± 20	220 ± 20	220 ± 20	220 ± 20
Error in prediction (%)	5	5	4	1.4

Linear regressions between TS and length have been shown in Table 3 and Table 4 for 120 kHz and 200 kHz respectively. To evaluate the performance of the prediction capabilities of such relationships we have focused on the linear regressions obtained at an orientation interval from -5° to 5° for both frequencies, and used a set of single traces extracted from the echograms without optical correspondence, that is, an independent set of acoustic data. 25,387 isolated traces at 120 kHz and 18,862 at 200 kHz were used, which had not been used to obtain the TS versus length linear regressions. The calculated tuna length values were compared with the harvested mean length values to evaluate the corresponding deviations in predictions (Table 5). In Table 5 we can see that the prediction error was always under 5 %, slightly more for uncompensated TS than for compensated TS. For compensated TS at 200 kHz, the error was reduced to <1.4 %.

3.3. Results of numerical simulations of target strength in the near field of Bluefin Tuna

The dependence of the simulated ventral TS on the distance from fish to the transducer was numerically assessed for swimbladder MFS models corresponding to tuna fork lengths of FL = 120 cm and FL = 225 cm. Results are shown in Fig. 13, where the estimated maximum TS values as a function of the distance from fish to transducer are depicted for both tuna lengths at the working frequency of 120 kHz. The computed maximum TS increases with distance. For the bigger fish, FL = 225 cm, at it has a variation of up to 6.5 dB between 1 and 20 m, but the main variation occurs in the first meters, with 5 dB between 1 and 5 m, with an asymptotic evolution towards the far field value afterwards. For

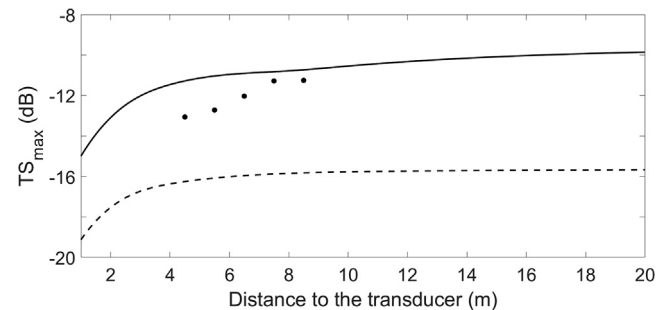


Fig. 13. Maximum TS calculated from the swimbladder model at f = 120 kHz for FL = 120 cm (solid) and FL = 200 cm and uncompensated TS measured for fork length between 220 and 230 cm at 120 kHz (dots).

the shorter fish, FL = 120 cm, the variation interval is less than 4 dB, the main change (3 dB) appearing in the first 4 m.

A comparison between numerically evaluated TS values and the experimentally measured TS is also shown in Fig. 13. The figure includes the computed maximum TS for the swimbladder model of a 225 cm fork length tuna, and the uncompensated maximum TS measured at 120 kHz for tuna with length between 220 and 230 cm (Fig. 12a).

3.4. Results of estimation of the influence of pulse duration on the target strength measurements

Once selected for our measurements the smallest available pulse duration of 64 μs, we calculated the estimated TS bias with the expression derived in section 2.7. The result is plotted in Fig. 6 as a function of Bluefin Tuna fork length (assuming the maximum horizontal and vertical dimensions for the swimbladder derived from section 2.7). It can be observed that the TS bias varies between -0.1 to -0.7 dB for fishes from 2.2 to 3 m long.

4. Discussion

This work was carried out in production conditions in a Bluefin fattening cage, so a great variety of tuna sizes were present in the cage; i.e. the population had a high variability in size. Single tuna biometric information was provided by a stereoscopic video system. In [15] the accuracy of the automatic stereoscopic measure-

ments were validated by comparing them with two ground truths: one configured with manual measurements and one with real SFL measurements of the tuna stock collected at harvesting. To configure the first ground truth, samples were measured manually by three different operators to obtain a mean value. The snout tip and the tail fork point were manually marked in the left image using the mouse pointer, whereas the corresponding right image points are also marked, but with the aid of the epipolar lines resulting from the stereo-vision calibration. Comparison with the manual measurements demonstrated that the system delivered good accuracy in terms of fish length estimation error (up to 50 % of the samples bounded in a 1 % error and up to 90 % of the samples bounded in a 3 % error). Real SFL measurements of the tuna stock were collected at harvesting to configure the second ground truth. When compared with real SFL measurements of the tuna stock, the system provided highly accurate length measurements, obtaining no statistically significant difference between automatic and real SFL frequency distributions. The optical measuring system limited the studied distance range to between 4 and 10 m from the sensors (cameras and transducers). One consequence of this range limitation was that only the tested 31° beam width could completely insonify a 2 m long tuna within that distance interval, whereas the 7° transducer could only cover the size of the corresponding swimbladder. Another consequence is related to the capability of isolating individual traces between these limits in the dense echograms obtained in the cited production conditions. Tuna traces appeared to be overlapped for the wider beam, even at the short range where the stereoscopic video could provide length measurements. The capability of automatic isolation of traces in the whole video measuring range was improved for the narrower beam and the shortest pulse duration (7° and $64 \mu\text{s}$), as seen in Fig. 7e and Table 2. Then, the maximum amplitude within the isolated trace was used to calculate the TS of the fish, assuming that more than 90 % of its value is due to this organ when present.

The choice of this configuration had other implications in terms of TS measurements. On one hand, a short pulse duration improves target distance determination when measurements are made near to the transducer [17] avoiding overestimation of the received echo level. Moreover, more accurately received echo compensation values using an asymptotic TVG function can be achieved using short pulse length [28]. On the other hand, the spatial resolution of such a pulse duration is about 5 cm in sea water, which was sufficient to resolve the contribution of the swimbladder for the ABFT studied (Fig. 8d), but it can introduce a bias on the measured TS for larger fishes. The estimated value of this bias is smaller than 1 dB even for the biggest caged fishes, being the typical standard deviations of TS distributions of the measured cages between 7 and 11 dB.

The exact definition of TS is not accomplished then for the bigger fishes, since (as mentioned above) the scatterer (the swimbladder) is not completely insonified inside the pulse volume. In spite of this fact, the obtained results permit us to predict tuna size with an error below 5 % for all cages under study. It must be mentioned that the estimated bias introduced by the short pulse duration is lower than 1 dB for all size classes, and thus its influence could be masked by the natural variability of swimbladder size and shape.

This is an interesting subject for discussion that can be common in the extension of the concept of TS measured with the new broadband echosounders with chirped signals [49,50], that perform a frequency sweep in the operating band. TS values are calculated as a function of frequency, and for each frequency step, the insonified volume is just a portion of the one corresponding to the total pulse duration. A natural continuation of this work is the acoustic characterisation of ABFT with a broadband system, taking advantage of a significantly improved spatial resolution provided by pulse compression.

Reducing fish TS to swimbladder TS also had the effect of reducing the fish's far-field distance, as can be observed in the numerical simulations plotted in Fig. 9a. The estimates of far field distance at 120 kHz for a 2 m long fish are beyond 80 m, whereas this distance is reduced to a slightly more than 3.2 m for the corresponding swimbladder size [51]. We can see in Fig. 9a that the main variation of TS due to near field effects, when also considering a realistic beam aperture, is found at distances below 5 m, with the variation inside the interval between 4 and 10 m lower than 1 dB in most cases. The experimental measurements are a bit higher, but in quite good agreement with the simulated values (Fig. 13), considering the approximate nature of the tuna swimbladder model, and the expected minor contribution from the tuna's flesh and bones (not computed).

The beam compensation provided narrower compensated TS distributions (for both frequencies), with significant reductions in CV (Fig. 9b and 9e). It is pertinent to discuss here whether beam directivity compensation makes sense with such an evident violation of the point-like nature of the scatterer, since even the bladder alone occupies a significant part of the total insonified beam volume. The results showed that the beam compensation results in an improvement of the TS to size correlation for 200 kHz with fish orientation limited between -5° and 5° , and -10° and 10° . For higher angular intervals in fish swimming tilt the correlations are poorer. For 120 kHz measurements, beam compensation directly does not make any beneficial contribution. We must underline that beam compensation is carried out only for the maximum TS value of the isolated fish trace, that it is a complex and it cannot be reduced to a single linear track (as explained in the previous section). Also, it must be noted that the fattening process could increase the variability of measured TS, because fat deposits in tuna bellies could produce a swimbladder masking effect depending on amount of fat. It is predicted that during the fattening process the fat deposits could increase more for bigger tuna than for smaller ones, causing wider distributions.

It is widely known that fish orientation contributes to the variability of the registered backscattered energy [52]. Different works have shown that tuna in captivity swim in an elliptical pattern with vertices at different heights so that the swimming path is greater [53–55]. Also, studies in tanks have reported non-symmetrical tuna swimming orientation; it was approximately -5° to 1° for YFT [22]. In addition, ABFT changes direction and vertical position in response to external stimuli [6,41,53], and this behaviour has been recorded by the stereoscopic video system during our experiments. All these factors, combined with the fixed position of the equipment in the cage, may explain the tilted average for the swimming direction measured (Fig. 10), and the broadening of the TS distributions.

The relationship between TS value and tuna orientation has been studied for YFT in situ [20] and in tanks [22]. Those works revealed that the maximum TS values are obtained when tuna swims a -25° tilt angle (such an angle implies the tuna is heading down), and swimbladder backscattering cross-section reaches a maximum. Given that the main amount of tuna measured in this work were within an orientation range from -5° to 5° (Fig. 10), we have not been able to clearly verify this effect of the tilted position of the swimbladder for ABFT.

The linear regression found for each frequency, taking into account all possible orientations (-35° to 35° interval), could be a tool to predict the mean length in the cage from acoustic data. The coefficient of determination is better for uncompensated TS than for compensated TS when all the orientations are included. This is an interesting feature when considering the possible use of single-beam echosounders, opening the door to lower cost equipment for checking on biomass in production conditions.

5. Conclusions and further work

Acoustic and stereoscopic video measurements in ABFT fattening cages were taken to find a relationship between TS and tuna fork length that could be used to evaluate tuna biomass. However, the production conditions increase the complexity for carrying out acoustic measurements. The synchronized use of acoustic and optic systems allows a TS value to be assigned a particular tuna. This technique simultaneously provides the TS value, fork length, orientation and distance to the sensors, but the measuring conditions do not allow data around the fish to be collected in the acoustic far field because of the tuna's dimensions, fish density, and the limited close distance range for optical measurement. Big targets could be measured in the far field of the acoustic transducers, but still too close with a limited insonified area; thus, uncertainties associated with near range measurements affected the TS values obtained. Nevertheless, the selected echosounding configuration reduced the expected effects, and lineal regressions between TS and tuna fork length have been obtained and studied. As the main conclusion, it can be stated that uncompensated values of TS correlate fairly well with the fish fork length without the need specify the tuna's tilt angle. When the fish orientation was reduced, better correlation between compensated TS and logarithmic ABFT fork length were obtained at 200 kHz.

Combined use of acoustic and optical techniques has enabled strong relationship to be established between TS and ABFT length in fattening cages. An operative tool to predict the mean tuna length in fattening cages from acoustic data has been presented, which may be a fundamental tool to improve the biomass estimation procedures for purse seiners' and tuna traps' catches. However, it is still necessary to study the TS values' accuracy and target response depending on fish condition. To do so, numerical simulations should include better information about swimbladder size, shape and situation with respect from tuna backbone. Also, the effects of the fattening process on the acoustic target response should be considered and new measurement campaigns carried out throughout an entire fattening cycle. New measurements with broadband techniques would be also desirable, increasing the resolution and the capability to differentiate the fishes' inner structures.

CRedit authorship contribution statement

V. Puig-Pons: Conceptualization, Software, Methodology, Investigation, Formal analysis, Writing – original draft. **P. Muñoz-Benavent:** Resources, Software, Methodology, Investigation, Formal analysis, Writing – original draft. **I. Pérez-Arjona:** Conceptualization, Methodology, Validation, Writing – original draft, Writing – review & editing, Visualization. **A. Ladino:** Validation, Data curation, Formal analysis. **S. Llorens-Escribà:** Investigation, Formal analysis. **G. Andreu-García:** Supervision, Project administration, Writing – review & editing. **José M. Valiente-González:** Conceptualization, Writing – review & editing. **V. Atienza-Vanacloig:** Conceptualization, Writing – review & editing. **P. Ordóñez-Cebrián:** Resources, Investigation, Writing – original draft. **José I. Pastor-Gimeno:** Formal analysis, Writing – review & editing. **V. Espinosa:** Conceptualization, Supervision, Project administration, Funding acquisition, Writing – original draft, Writing – review & editing.

Declaration of Competing Interest

The authors declare the following financial interests/personal relationships which may be considered as potential competing interests: Vicente Puig-Pons has patent "Method for determining

tuna biomass in a water zone and corresponding system" issued to Balfego & Balfego S.L, et al.

Acknowledgements

This work was supported by funding from the ACUSTUNA project ref. CTM2015-70446-R (MINECO/ERDF, EU). The authors are grateful for the support provided by Grup Balfegó for their collaboration and implication in installing and maintaining of the experimental setup in their tuna cages at l'Ametlla de Mar and for providing an ABFT specimen for x-ray imaging.

References

- [1] ICCAT, 2019. Recommendation by ICCAT amending the Recommendation 18-02 establishing a multi-annual management plan for Bluefin tuna in the eastern Atlantic and the Mediterranean. Ihlenburg, F. 1998. Finite Element Analysis of Acoustic Scattering, Applied Mathematical Sciences (Springer-Verlag, New York), Vol. 132, 182 pp.
- [2] FAO. 2020. The State of World Fisheries and Aquaculture 2020. Sustainability in action. Rome. 10.4060/ca9229en.
- [3] FAO. 2021. Fisheries and aquaculture statistics. World aquaculture production 1950–2019 (Fishstat). FAO Fisheries Division. Rome. Update 2021. www.fao.org/fishery/statistics/software/fishstatj/en.
- [4] De la Gándara F, Ortega A, Buentello A. 2016. "Tuna Aquaculture in Europe." Advances in Tuna Aquaculture. From hatchery to market, edited by L. Benetti, D.D., G.J. Partridge and A. Buentello (Eds). Elsevier Academic Press.
- [5] Aguado F, García B. 2006. "Estimación de La Biomasa En Especies En Cultivo Por Métodos No Invasivos: Adecuación Y Puesta a Punto de Las Técnicas Para Diversas Especies En El Atlántico Y El Mediterráneo." Junta Nacional Asesora de Cultivos marinos (JACUMAR) y Ministerio de Agricultura, Pesca y Alimentación.
- [6] Puig-Pons, V. 2017. "Control y Caracterización del atún rojo en jaulas marinas." Tesis Docotral. edited by Universitat Politècnica de València. Universitat Politècnica de València.
- [7] Phillips K, Rodriguez VB, Harvey E, Ellis D, Seager J, Begg G, Hender J. 2009. Assessing the operational feasibility of stereo-video and evaluating monitoring options for the Southern Bluefin Tuna Fishery ranch sector, Fisheries Research and Development Corporation and Bureau of Rural Sciences (Australia). Report 2008/44, ISBN 978-1-921192-32-6.
- [8] Shieh ACR, Petrell RJ. Measurement of fish size in atlantic salmon (*salmo salar* L.) cages using stereographic video techniques. *Aquacult Eng* 1998;17:29–43.
- [9] Costa C, Loy A, Cataudella S, Davis D, Scardi M. Extracting fish size using dual underwater cameras. *Aquacult Eng* 2006;35:218–27.
- [10] Costa C, Scardi M, Vitalini V, Cataudella S. 2009. A dual camera system for counting and sizing Northern Bluefin Tuna (*Thunnus thynnus*, Linnaeus, 1758) stock, during transfer to aquaculture cages, with a semi-automatic Artificial Neural Network tool. *Aquaculture*, 291: 161–167. Elsevier B.V.
- [11] Katavić I, Šegvić-Bubić T, Grubišić L, Talijančić I. 2016. Reliability of Bluefin Tuna Size Estimates Using A Stereoscopic Camera System. *Collective Volume of Scientific Papers ICCAT 72*: 1848–1861.
- [12] Shafait F, Harvey ES, Shortis MR, Mian A, Ravanbakhsh M, Seager JW, et al. Towards automating underwater measurement of fish length: a comparison of semi-automatic and manual stereo- video measurements. *ICES J Mar Sci* 2017;10-1093.
- [13] Muñoz-Benavent P, Andreu-García G, Valiente-González JM, Atienza-Vanacloig V, Puig-Pons V, Espinosa V. Automatic Bluefin Tuna sizing using a stereoscopic vision system. *ICES J Marine Sci* 2018;75:390–401.
- [14] Atienza-Vanacloig V, Andreu-García G, López-García F, Valiente-González JM, Puig V. Vision-based discrimination of tuna individuals in grow-out cages through a fish bending model. *Comput Electron Agric* 2016;130:142–50.
- [15] Muñoz-Benavent P, Andreu-García G, Valiente-González JM, Atienza-Vanacloig V, Puig-Pons V, Espinosa V. Enhanced fish bending model for automatic tuna sizing using computer vision. *Comput Electron Agric* 2018;150:52–61.
- [16] Simonds J, MacLennan D. 2007. *Fisheries Acoustics: Theory and Practice* Second Edition. Second edi. edited by D. Simonds, J, MacLennan. Blackwell Science.
- [17] Foote K, Knudsen H, Vestnes G, MacLennan D, Simmonds E, 1987. "Calibration of Acoustic Instruments for Fish Density Estimation: A Practical Guide." International Council for the Exploration of the Sea.
- [18] Furusawa M. Prolate spheroidal models for predicting general trends of fish target strength. *J Acoust Soc Jpn (E)* 1988;9:13–4.
- [19] Love RH. Dorsal-aspect target strength of an individual fish. *J Acoust Soc Am* 1971;49(3B):816–23.
- [20] Bertrand A, Josse E, Masse J. In situ acoustic target-strength measurement of bigeye (*Thunnus obesus*) and yellowfin tuna (*Thunnus albacares*) by coupling split-beam echosounder observations and sonic tracking. *ICES J Mar Sci* 1999;56(1):51–60.
- [21] Bertrand A, Josse E. Tuna target-strength related to fish length and swimbladder volume. *ICES J Mar Sci* 2000;57(4):1143–2116.

- [22] Hsueh-Jung L, Myounghee K, Hsing-Han H, Chi-Chang L, Long-Jin W. Ex situ and in situ measurements of juvenile yellowfin tuna *Thunnus albacares* target strength. *Fish Sci* 2011;77(6):903–13.
- [23] Melvin GD. Observations of in situ Atlantic bluefin tuna (*Thunnus thynnus*) with 500-kHz multibeam sonar. *ICES J Mar Sci* 2016;73:1975–86.
- [24] Knudsen FR, Fosseidengen JE, Oppedal F, Karlsen O, Ona E. Hydroacoustic monitoring of fish in sea cages: target strength (TS) measurements on Atlantic Salmon (*Salmo Salar*). *Fish Res* 2004;69(2):205–9.
- [25] MacLennan DN. Time varied gain functions for pulsed sonars. *J Sound Vibrat* 1986;110(3):511–22.
- [26] Furusawa M, Hamada M, Aoyama C. Near range errors in sound scattering measurements of fish. *Fisheries Science: FS* 1999;65(1):109–19.
- [27] Dawson JJ, Wiggins D, Degan D, Geiger H, Hart D, Adams B. Point-source violations: split-beam tracking of fish at close range. *Aquat Living Resour* 2000;13(5):291–325.
- [28] Moszyński M, Stepnowosky A. Increasing the accuracy of time-varied gain in digital echosounders. *Acta Acustica United with Acustica* 2002;88(5):814–7.
- [29] Pérez-Arjona I, Godinho L, Espinosa V. Numerical simulation of target strength measurements from near to far field of fish using the method of fundamental solutions. *Acta Acustica United with Acustica* 2018;104(1):25–38.
- [30] Cort JL, Deguara E, Galaz E, Mèlich B, Artetxe I, Arregi I, et al. Determination of L Max for Atlantic Bluefin Tuna, *Thunnus Thynnus* (L.), from meta-analysis of published and available biometric data. *Rev Fish Sci* 2013;21(2):181–212.
- [31] Rodríguez-Sánchez V, Encina-Encina L, Rodríguez-Ruiz A, Sánchez-Carmona R. Do close range measurements affect the target strength (TS) of fish in horizontal beaming hydroacoustics? *Fish Res* 2016;173:4–10.
- [32] Anderson VC. Sound scattering from a fluid sphere. *J Acoust Soc Am* 1950;22:426–31.
- [33] Stanton TK, Chu D, Wiebe PH. Sound scattering by several zooplankton groups II: Scattering models. *J Acoust Soc Am* 1998;103:236–53.
- [34] Foote KG. Rather-high-frequency sound scattering by swimbladdered fish. *J Acoust Soc Am* 1985;78:688–700.
- [35] Foote KG, Francis DTI. Comparing Kirchhoff approximation and boundary-element models for computing gadoid target strengths. *J Acoust Soc Am* 2002;111:1644–54.
- [36] Francis DTI. A gradient formulation of the Helmholtz integral equation for acoustic radiation and scattering. *J Acoust Soc Am* 1993;93:1700–9.
- [37] Francis DTI, Foote KG. Depth-dependent target strengths of gadoids by the boundary-element method. *J Acoust Soc Am* 2003;114:3136–46.
- [38] Jech JM, Horne JK, Chu D, Demer DA, Francis DTI, Gorska N, et al. Comparisons among ten models of acoustic backscattering used in aquatic ecosystem research. *J Acoust Soc Am* 2015;138:3742–64.
- [39] Macaulay GJ, Peña H, Fässler SMM, Pedersen G, Ona E. Accuracy of the Kirchhoff-approximation and Kirchhoff-raymode fish swimbladder scattering models. *PLoS ONE* 2013;8:e64055.
- [40] Simrad, 2008. "Simrad ER60, Scientific Echo Sounder. Reference Manual."
- [41] Sarà G, Buffa G, Lo Matire M. Effect of boat noise on the behaviour of bluefin Tuna *Thunnus Thynnus* in the Mediterranean Sea. *Mar Ecol Prog Ser* 2007;331 (February):243–53.
- [42] Schaefer, K. M. and Oliver, C. W. 1998. Shape, Volume, and Resonance Frequency of the Swimbladder of Yellowfin Tuna (*Thunnus albacares*). National Marine Fisheries. Service Southeast Fisheries Science Center. P.O. Box 271. La Jolla, CA 92038. Center. P.O. Box 271. La Jolla, CA 92038.
- [43] Aguado-Gimenez F, Garcia-Garcia B. 2005. Growth, food intake and feed conversion rates in captive Atlantic bluefin tuna (*Thunnus thynnus* Linnaeus, 1758) under fattening conditions. *Aquaculture Research*, 36: 610–614. Blackwell Science Ltd.
- [44] Puig-Pons V, Estruch VD, Espinosa V, De la Gándara F, Melich B, Cort JL. Relationship between weight and linear dimensions of Bluefin tuna (*Thunnus thynnus*) following fattening on western Mediterranean farms. *PLoS ONE* 2018;13(7):e0200406.
- [45] Puig-Pons V, Estruch VD, Espinosa V, de la Gándara F, Melich B, Cort JL. Correction: Relationship between weight and linear dimensions of Bluefin tuna (*Thunnus thynnus*) following fattening on western Mediterranean farms. *PLoS ONE* 2021;16(10):e0259437.
- [46] McClatchie S, Macaulay G, Coombs R. A requiem for the use of 20 log10 length for acoustic target strength with special reference to deep-sea fishes. *ICES J Marine Sci: J Du Conseil* 2003;60(2):419–28.
- [47] Lurton X. 2002. *An Introduction to Underwater Acoustics: Principles and Applications*. Springer-Verlag, pp 347.
- [48] Gaunaurd CG. "Sonar cross sections of bodies partially insonified by finite sound beams", *IEEE J. Oceanic Eng.*, vol. OE-10, pp. 213–230, July 1985.
- [49] Chu D, Stanton TK. Application of pulse compression techniques to broadband acoustic scattering by live individual zooplankton. *J Acoustical Soc Am* 1998;104:39–55.
- [50] Chu D, Eastland GC. Calibration of a broadband acoustic transducer with a standard spherical target in the near field. *J Acoustical Soc Am* 2015;137:2148–57.
- [51] Medwin H, Clay CS. *Fundamentals of acoustical oceanography*. Boston: Academic Press; 1998. p. 712.
- [52] Dahl PH, Mathisen OA. Measurement of fish target strength and associated directivity. *J Acoust Soc Am* 1983;73(4):1205–11.
- [53] Nucci ME, Costa C, Scardi M, Cataudella S. Preliminary observations on Bluefin Tuna (*Thunnus Thynnus*, Linnaeus 1758) behaviour in captivity. *J Appl Ichthyol* 2010;26:95–8.
- [54] Komeyama K, Kadota M, Torisawa S, Suzuki K, Tsuda Y, Takagi T. Measuring the swimming behaviour of a reared Pacific Bluefin Tuna in a submerged aquaculture net cage. *Aquat Living Resour* 2011;24(2):99–105.
- [55] Komeyama K, Kadota M, Torisawa S, Takagi T. Three-dimensional trajectories of cultivated Pacific Bluefin Tuna *Thunnus Orientalis* in an aquaculture net cage. *Aquaculture Environ Interact* 2013;4(1):81–90.